Nanostructures

Deutsche Ausgabe: DOI: 10.1002/ange.201605317
Internationale Ausgabe: DOI: 10.1002/anie.201605317

Formation and Reversible Morphological Transition of Bicontinuous Nanospheres and Toroidal Micelles by the Self-Assembly of a Crystalline-*b*-Coil Diblock Copolymer

*David Presa-Soto, Gabino A. Carriedo, Raquel de la Campa, and Alejandro Presa Soto**

Abstract: *We herein report the formation of two complex nanostructures, toroidal micelles and bicontinuous nanospheres, by the self-assembly of the single structurally simple crystalline-b-coil diblock copolymer poly[bis(trifluoroethoxy)phosphazene]-b-poly(styrene), PTFEP-b-PS, in one solvent (THF) and without additives. The nature of these nanostructures in solution was confirmed by DLS and cryo-TEM experiments. The two morphologies are related by means of a new type of reversible morphological evolution, bicontinuous-to-toroidal, triggered by changes in the polymer concentration. WAXS experiments showed that the degree of crystallinity of the PTFEP chains located at the core of the toroids was higher than that in the bicontinuous nanospheres, thus indicating that the final morphology of the aggregates is mostly determined by the ordering of the PTFEP core-forming blocks.*

The self-assembly of amphiphilic block copolymers (BCPs) has been demonstrated as an invaluable tool for the construction of well-defined nanostructures.[1] Besides the classical nanomorphologies created by this methodology (spheres, cylinders, or bilayer membranes),[1,2] nanotoroids (donut- or ring-shaped) and bicontinuous nanospheres have become textures of special interest owing to their rarity, complexity, and importance in some technological and biological processes. For instance, Nature uses nanotoroidal morphologies during DNA packaging (DNA condensation)[3] and in some viruses and sperm cells.[4] Toroids are also very important in the design of artificial delivery systems for gene therapy.[5] On the other hand, micelles with internal bicontinuous structures are considered promising carriers for the simultaneous inclusion of chemically different encapsulated drugs and of interest for their possible catalytic and templating properties.[6] Since pioneering studies on the synthesis of toroidal[7] and bicontinuous nanostructures[8] from the self-assembly of BCPs, very few examples of toroidal (mixed with other morphologies)[9] and bicontinuous[10] micelles derived from BCPs have been reported, mostly from chemically and structurally rather complex combinations of blocks. However, these two morphologies have also been produced purely from simple linear block copolymers,[11] thus demonstrating that structural complexity is not a necessary condition for their formation.

The self-assembly of block copolymers containing a crystallizable core-forming block and a random-coil block (crystalline-*b*-coil BCPs) has been exploited to create complex nanomorphologies by crystallization-driven living self-assembly.[12] Recently, our group has demonstrated the synthesis of reversibly responsive (to changes in pH) giant unilamellar vesicles (GUVs) by the self-assembly of the BCPs $[N{=}P(OCH_2CF_3)_2]_n$-*b*-$[N{=}PMePh]_m$ containing crystalline $[N{=}P(OCH_2CF_3)_2]$ segments.[13] Herein we report a new and convenient synthesis of the hybrid crystalline-*b*-coil poly[bis(trifluoroethoxy)phosphazene]-*b*-polystyrene (PTFEP-PS) by the use of lithiated initiators functionalized with phosphine groups (Scheme 1). The self-assembly of these polymers in THF without additives or cosolvents led to pure toroidal micelles or bicontinuous nanospheres depending on the polymer concentration. Moreover, these rare morphologies can be reversibly created one from the other in solution by a bicontinuous-to-toroidal morphological transition observed during this study for the first time.

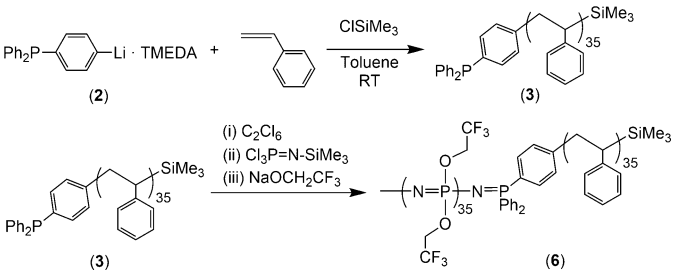

Scheme 1. Synthesis of BCP **6**. Reaction conditions (see the Supporting Information for details): i) RT/CH_2Cl_2/12 h; ii) RT/CH_2Cl_2/14 h; iii) RT/THF/12 h. TMEDA = *N*,*N*,*N*′,*N*′-tetramethylethylenediamine.

Linear $PTFEP_{35}$-PS_{35} (**6**, PDI = 1.1, the numbers in subscript refer to the number-average degree of polymerization of each block) was synthesized by using the lithiated phosphine **2** as an initiator of the anionic polymerization of styrene in toluene at room temperature (RT = 20 °C; see Scheme 1 and Scheme S1 in the Supporting Information for further details). The initiator **2** was generated in situ by the treatment of (4-bromophenyl)diphenylphosphane (**1**) with *tert*-butyllithium (2 equiv) in the presence of TMEDA

[*] D. Presa-Soto, Prof. G. A. Carriedo, Dr. R. de la Campa, Dr. A. Presa Soto
Facultad de Química, Química Orgánica e Inorgánica (IUQOEM)
Universidad de Oviedo
Julián Clavería s/n, 33006 Oviedo (Spain)
E-mail: presaalejandro@uniovi.es

Supporting information for this article, including experimental procedures and characterization details of polymers **3** and **4** and BCPs **5** and **6**, DLS of BCP **6** at different concentrations in THF, WAXS of bulk samples of PS_{35}-PPh_2 (**3**) and $PTFEP_{35}$ homopolymer, and all self-assembly procedures, as well as the ORCID identification number(s) for the author(s) of this article can be found under http://dx.doi.org/10.1002/anie.201605317.

(1 equiv; see the Supporting Information). The complete lithiation of **1** was checked by treating a freshly prepared solution of **2** with $ClSiMe_3$ at room temperature (20 °C) and confirming the quantitative formation of [(4-trimethylsilyl)-phenyl]diphenylphosphane (**7**; see the Supporting Information) and the total absence of **1** by ^1H, ^{13}C, and ^{31}P NMR spectroscopy. When styrene (35 equiv) was quickly added to a solution of **2** (1 equiv) in toluene at room temperature, the telechelic polystyrene **3** (PS_{35}-PPh_2, $M_n = 3915$, PDI = 1.1; see the Supporting Information) was obtained after quenching the reaction with $ClSiMe_3$. The chlorination of **3** with C_2Cl_6 led to PS_{35}-PPh_2Cl_2 (**4**), which has $-PPh_2Cl_2$ end groups that initiate the polymerization of $Cl_3P{=}NSiMe_3$[14] to give the block copolymer $[N{=}PCl_2]_{35}$-PS_{35} (**5**; see the Supporting Information). The macromolecular substitution of the chlorine atoms by $-OCH_2CF_3$ groups led to the block copolymer $PTFEP_{35}$-PS_{35} (**6**) containing crystalline $[N{=}P(OCH_2CF_3)_2]$ blocks. This synthetic methodology afforded **6** in similar yield (63 %) and with similar narrow polydispersities (PDI = 1.2; see the Supporting Information) to those of the previous method,[15] but by a significantly simpler experimental procedure (only the intermediate polymer **3** was isolated and purified (see Scheme S1), whereas the other method requires the isolation of three different polymer intermediates).

On the basis of our previous study, in which THF was used as a solvent for the crystallization of $[N{=}P(OCH_2CF_3)_2]$ blocks in the capsule wall of giant vesicles,[13] aggregates of **6** were induced by dissolving the block copolymer (1 mg) in THF (3 mL) at room temperature (note that the solubility parameters, $\delta\,(MPa^{1/2}) = 18.6$ (THF),[16] 18.6 (PS),[16] and 19.6 (PTFEP),[17] indicate that THF is a better solvent for the PS than for the PTFEP) and subjecting the solution to sonication for 2 min at 20 °C (see the Supporting Information). The resulting translucent solution of **6** was first investigated by dynamic light scattering (DLS; see Figure S8). The solution was aged at room temperature until the apparent hydrodynamic radius ($R_{h,app}$) of the aggregates reached a constant value of 74 nm (dispersity 0.332) after 24 h. High-resolution transmission electron microscopy (HRTEM) demonstrated that spherical aggregates were present at room temperature with a number-average diameter, D_n, of 112 nm (N (number of objects) = 125), and $D_w/D_n = 1.5$ (see Figure 1 a). The micrographs showed that the aggregates had a nonhomogeneous structure, as revealed by the different contrast regions. To examine the morphological features of these aggregates, we stained the samples with RuO_4 (selective staining for the PS block containing aromatic rings). We found that the spherical structure was composed of interconnected screwlike worm-shaped segments, the space between them corresponding to the low-contrast regions in the HRTEM images (Figure 1 b).

To verify that the bicontinuous structure was created in solution (i.e. during the self-assembly processes) rather than after drop-casting (i.e. during drying or solvent evaporation), we performed cryo-TEM experiments on the solution of **6** in THF. The micrographs clearly displayed spherelike particles ($D_n = 95$ nm, $D_w/D_n = 1.8$, $N = 30$) with a rather bicontinuous networklike internal structure (Figure 1 c, d). However, some of the bicontinuous aggregates also exhibited regions with

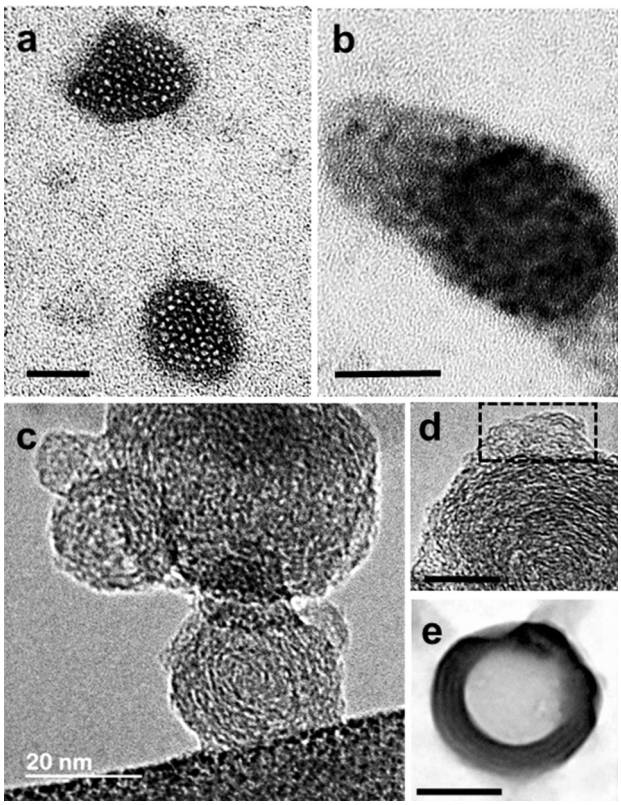

Figure 1. a, b) Bright-field HRTEM images of aggregates from BCP **6** in THF (0.33 mg mL^{-1}) without staining with RuO_4 (a), and after staining with RuO_4 (b). Scale bars correspond to 50 nm. c, d) Cryo-TEM images of aggregates from BCP **6** in THF (0.33 mg mL^{-1}) showing their bicontinuous structure (c) and regions of disordered lamella structure (area inside the dashed rectangle; d). Scale bar in (d) corresponds to 50 nm. e) Bright-field HRTEM of a multilamellar vesicle formed from BCP **6** in THF with 1.6 vol % water (final concentration of **6** in the solution: 0.33 mg mL^{-1}). Scale bar corresponds to 200 nm.

disorder or twisted lamellar phases (see region within the dashed lines in Figure 1 d) similar to that previously reported by Sommerdijk and co-workers.[11a] Thus, the cryo-TEM experiments demonstrated unambiguously that the bicontinuous structure of the nanospheres was created in solution during the self-assembly of **6** and not during drying. Under these self-assembly conditions ($C = 0.33$ mg mL^{-1}), the balance between the larger volume occupied by the swollen PS chains and that of the less swollen PTFEP in THF (see values of $\delta\,(MPa^{1/2})$) imposes a negative curvature on the aggregates that, because of the core microphase segregation, leads to spherelike micelles with bicontinuous inner structures. It is known that enhanced segregation can be obtained in block copolymers by inserting fluorine into one of the blocks,[18] and that this approach offers a route to structured micelles.[19] Therefore, in BCP **6**, the high cohesive energies between the $[N{=}P(OCH_2CF_3)_2]$ blocks, which trigger their immiscibility with both the polystyrene block and the solvent, facilitate the core microphase separation leading to bicontinuous nanospheres. When the self-assembly was studied at the same concentration (0.33 mg mL^{-1}) but in cyclohexane at room temperature ($\delta\,(MPa^{1/2}) = 16.8$,[16] still a good solvent for the

PS but a poor solvent for PTFEP), the cryo-TEM image (after 24 h) showed the presence of poorly defined spherical micelles with no evidence of a bicontinuous structure (see Figure S9).

As the specific conditions to produce bicontinuous nanospheres are very difficult to achieve,[10] no other bicontinuous nanospheres originating in the absence of additives, cosolvents, and/or structurally complex polymeric structures (i.e. from a linear block copolymer) have been synthesized previously, to the best of our knowledge. Instead, all reported bicontinuous nanospheres have been obtained from mixtures of an organic solvent and water.[11a] Moreover, the synthesis of bicontinuous or lamellar structures is possible by the selective variation of the affinity of the solvent for the constituent blocks.[11a] Therefore, we studied the effects of the presence of water on the structure of the bicontinuous aggregates formed by BCP **6**. When water (50 μL, 0.16 vol %) was added to the solution of **6** at a concentration of 0.33 mg mL^{-1} in THF (3 mL) at room temperature (this amount of water does not change the block-polymer concentration significantly), DLS after 24 h showed aggregates ($R_{h,app}$ = 175 nm, PDI = 0.356; see Figure S8) that were larger than those observed in pure THF. These aggregates were studied by HRTEM, which showed the presence of multilamellar vesicles (D_n = 250 nm, D_w/D_n = 1.6, N = 70; see Figure 1e). According to the δ (MPa$^{1/2}$) values of both blocks (18.6 (PS) and 19.6 (PTFEP)) and those of the solvents (18.6 (THF) and 47.9 (H_2O)[16]), THF is a better solvent for PS than for PTFEP, and water is very poor solvent for both. Therefore, the addition of water alters the balance between the excluded volumes of the PS and PTFEP blocks, thus leading to a similar volume occupation in the THF/water mixture, and a lamellar instead of a bicontinuous structure. The addition of the same amount (0.16 vol %) of cyclohexane (a good solvent for PS but poor for PTFEP) or MeOH (a good solvent for PTFEP but poor for PS) did not alter the balance between the excluded volumes of the PS and PTFEP blocks with respect to those in THF, thus resulting in bicontinuous nanospheres (see Figure S10).

When the concentration of BCP **6** was raised from 0.33 to 2 mg mL^{-1} (1 mg of **6** in 3 mL of THF), DLS (after 24 h at room temperature) showed a significant increase in $R_{h,app}$ from 74 to 125 nm (see Figure S8). The observation of these aggregates by HRTEM and SEM revealed the exclusive presence of pure and regular (in size and shape) toroidal micelles (donut- or ring-shaped; Figure 2a). Line energy-dispersive X-ray analysis (EDX) of the composition distribution of these micelles (Figure 2b, F in red, N in green, and P in blue) demonstrated the presence of toroidal nanostructures, in which the F, N, and P atoms were only detected in the dark rings and not in the center of the nanostructures. Cryo-TEM experiments (Figure 2c) confirmed the formation of the toroidal micelles in solution before the evaporation of the solvent on the solid substrate used for the TEM and SEM. Micelles were also investigated by AFM (on a mica disk; Figure 2d). The average diameter $2R$ of the toroid, as determined from the peak-to-peak distance in Figure 2e, was 130 nm, and the ring width ($2r$) 60 nm, which was very similar to the height of the nanostructure, 65 nm, thus

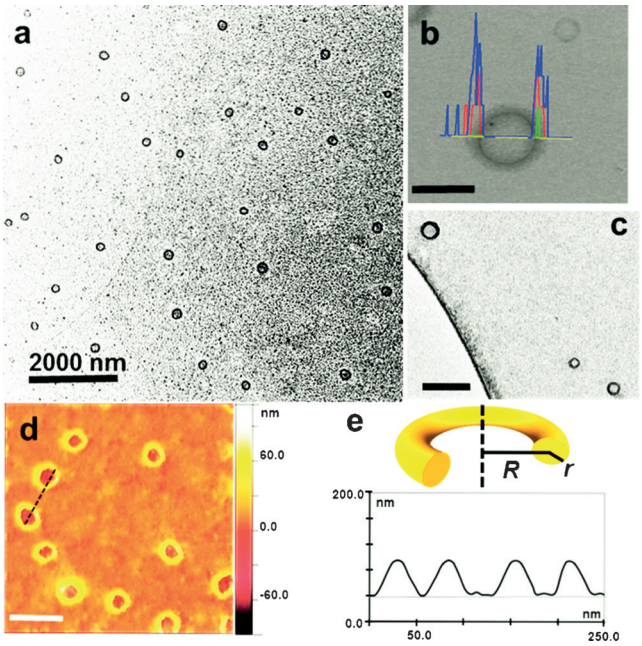

Figure 2. a) Bright-field HRTEM images of toroidal micelles from a 2 mg mL^{-1} solution of BCP **6** in THF. b) EDX line analysis (F in red, N in green, and P in blue) along the yellow line (inset). Scale bar corresponds to 200 nm. c) Cryo-TEM images of toroidal micelles from a 2 mg mL^{-1} solution of BCP **6** in THF. Scale bar corresponds to 200 nm. d) AFM height image of toroidal micelles. Scale bar corresponds to 100 nm. e) Depiction of the geometric parameters of the toroid and AFM cross-sectional height profiles across two micelles.

confirming the perfect toroidal shape. The calculated R_g value for our ring-shaped micelles is 140 nm ($R_g = R[1 + (3Z^2/4)]^{1/2}$, $Z = R/r$, with R = 65 nm, $2r$ = 60 nm, both calculated by AFM; Figure 2b), and the value of R_h = 126 nm (DLS), which gives the ratio R_g/R_h = 1.1. This value (1.1) is in very good agreement with the expected value (1.06) for a toroidal object.[11b] Again, when cyclohexane was used as a solvent (2 mg mL^{-1}), ill-defined spherical micelles were observed (see Figure S9).

The generation of bicontinuous nanospheres and toroidal micelles from the same linear BCP **6** by simply adjusting its concentration is of particular importance owing to the simplicity of the experimental methodology. Furthermore, we found that these two rare morphologies can be reversibly transformed one into the other. Thus, THF (5.0 mL) was added (over 15 min) to a solution of **6** in THF containing toroidal micelles (2 mg of **6** in 1 mL of THF, C = 2 mg mL^{-1}) with slow magnetic stirring to reach a final concentration of 0.33 mg mL^{-1} (see the Supporting Information). The solution was aged for 24 h (without stirring) and analyzed by DLS (see Figure S8). A decrease in the value of the $R_{h,app}$ from 126 (C = 2 mg mL^{-1}) to 80 nm (C = 0.33 mg mL^{-1}) was observed. Both HRTEM and cryo-TEM (see Figure S2) confirmed the presence of bicontinuous nanospheres with the same structure as that obtained when 1 mg of **6** was dissolved in 3 mL of THF. When the solution containing the bicontinuous nanospheres was slowly evaporated (with slow magnetic stirring under a flow of N_2(g) in a bath at 20 °C to avoid the cooling down of the solution) to reach a concentration of 2 mg mL^{-1}

(i.e. a final THF volume of 1 mL), the toroidal micelles were reconstructed (see Figure S2). He and Schmid demonstrated theoretically that pure toroidal micelles (i.e., exclusively with a toroidal shape) can be created by the self-assembly of a single component diblock copolymer (A-*b*-B) in the presence of a single solvent (S).[20] They proposed a non-conventional coalescent pathway, named growth mechanism, as the most likely pathway to lead to toroidal micelles. This mechanism involves the presence of bicontinuous aggregates as intermediates. Thus, our results, to the best of our knowledge, serve as the first experimental evidence of a morphological bicontinuous-to-toroid evolution triggered by the BCP concentration. Moreover, they give experimental support to the theoretically predicted growth mechanism in the formation of toroidal micelles from the self-assembly of BCPs.

To examine the influence of the crystallinity of the core-forming $[N{=}P(OCH_2CF_3)_2]$ blocks, we performed wide-angle X-ray scattering (WAXS) analysis of bulk samples of block copolymers **6** (as obtained after precipitation from solutions in THF into hexanes) and dried films containing the bicontinuous nanospheres and toroidal micelles (see the Supporting Information) resulting from their self-assembly (Figure 3). The WAXS experiments at room temperature of

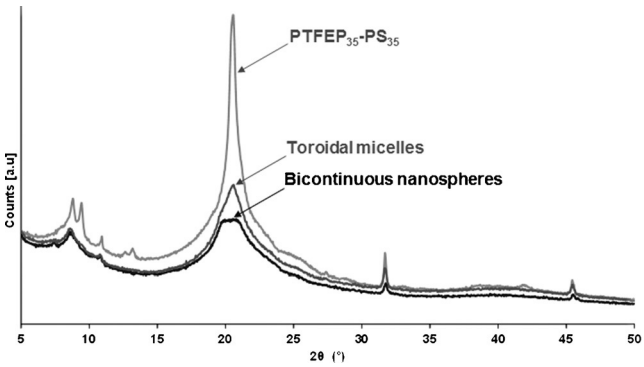

Figure 3. WAXS diffractograms for block copolymers **6** in the bulk prior to self-assembly experiments, and for dried toroidal micelles and bicontinuous nanospheres of BCP **6** after self-assembly in THF (at 2 and 0.33 mg mL^{-1}, respectively).

the bulk samples of **6** showed the reflections of the crystalline domains ($2\theta = 10.9$, 12.9, 20.8, 31.7, and 45.2°) and the characteristic signals corresponding to mesomorphic phases ($2\theta = 9.02°$ [$d = 9.80$ Å]), characteristic of the $[N{=}P(OCH_2CF_3)_2]$ homopolymer[21] (see Figure S11 for the WAXS analysis of PS_{35}-PPh_2 (**3**) and PTFEP with the same repeating units as those in the BCP **6**).

By the integration of the relative areas corresponding to the amorphous and crystalline domains in WAXS, the degree of crystallinity (*DC*) of the PTFEP block in bulk samples of BCP **6** was estimated as 31% (see Figure S12). The same reflections were present in the diffractogram of the dried films of both the bicontinuous and the toroidal aggregates (Figure 3). This result confirmed the location of the $[N{=}P(OCH_2CF_3)_2]$ in the core of the aggregates (crystalline order must correspond to the core and not to corona). However, as shown in Figure 3, the degree of crystallinity of the $[N{=}P(OCH_2CF_3)_2]$ segments in the toroidal micelles (8%) was higher than that in the bicontinuous nanospheres (< 1%; both values were estimated by integration of the relative areas corresponding to the amorphous and crystalline domains in WAXS; see Figure S12). These results might explain the dependence of the morphology on the BCP concentration. In fact, at high dilutions (i.e. 0.33 mg mL^{-1}), the crystallization of the $[N{=}P(OCH_2CF_3)_2]$ blocks is hampered by the swelling of the chains in THF, thus facilitating the core microphase separation that leads to the bicontinuous structures (the synthesis of bicontinuous morphologies in confined spaces has been predicted and observed in block copolymers previously[10]). On the other hand, when the concentration of BCP **6** is raised to 2 mg mL^{-1}, the crystallization of the $[N{=}P(OCH_2CF_3)_2]$ blocks favors the stability of the toroidal morphology. Thus, although crystallinity is not a key factor in the formation of bicontinuous nanospheres (as also observed with amorphous BCPs systems[11a]), these results suggest that the rigidity induced by the crystallization of the $[N{=}P(OCH_2CF_3)_2]$ blocks is crucial for the stabilization of toroidal morphologies.

In conclusion, we have shown that bicontinuous nanospheres or toroidal micelles can be obtained by the self-assembly of a single crystalline-*b*-coil poly-[bis(trifluoroethoxy)phosphazene]-*b*-poly(styrene) BPC in a single solvent (THF) without additives, by simply adjusting the BCP concentration. Moreover, these two rare morphologies can be reversibly transformed one into the other in THF by simple dilution (adding THF) or concentration (evaporating THF) of the BCP solution, thus establishing an unprecedented reversible morphological transition between bicontinuous nanospheres and toroidal micelles. This very important step in the growth mechanism operating in the creation of toroids has been experimentally demonstrated for the first time in this study. WAXS analysis of dried films containing bicontinuous or toroidal aggregates showed that whereas the PTFEP blocks are essentially amorphous in the structure of the bicontinuous nanospheres ($DC < 1\%$), the crystallization of those blocks in the core of the toroidal micelles ($DC = 8\%$) is crucial for the stability of these morphologies. Thus, the crystallinity of the core-forming $[N{=}P(OCH_2CF_3)_2]$ blocks appears to be the main guide to the creation of bicontinuous nanospheres and toroidal micelles. Thus, we can control the self-assembly of a single linear PTFEP-PS BCP to create bicontinuous or toroidal micelles by modulating the crystallization of the PTFEP segments by simply changing the BCP concentration. Currently, we are investigating the self-assembly of BCP **6** at different concentrations to establish relationships between the morphology and the degree of crystallization of the PTFEP blocks and to gain insight into the mechanism of the observed morphological evolution of bicontinuous nanospheres into toroidal micelles.

Acknowledgements

We thank the FICYT (Projects SV-PA-13-ECOEMP-83 and FC-15-GRUPIN14-106), Universidad de Oviedo (Project

UNOV-13-EMERG-GIJON-08), and the MINECO (Project CTQ2014-56345-P) for funding. We are also grateful to the COST Action Smart Inorganic Polymers (SIPs-CM1302—http://www.sips-cost.org/home/index.html). A.P.S. thanks the MEC for funding by the Juan de la Cierva and Ramón y Cajal programs. DPS is grateful to the MEC for an FPU grant. We are grateful to M. Avella (University of Valladolid, Spain) and Zakariae Amghouz (University of Oviedo) for their support with the cryo-TEM and HRTEM experiments.

Keywords: bicontinuous nanospheres · block copolymers · polyphoshazenes · self-assembly · toroidal micelles

How to cite: *Angew. Chem. Int. Ed.* **2016**, *55*, 10102–10107
Angew. Chem. **2016**, *128*, 10256–10261

[1] a) M. Lazzari, G. Liu, S. Lecommandoux, *Block Copolymers in Nanocience*, Wiley-VCH, Weinheim, **2006**; b) M. Lazzari, M. A. López-Quintela, *Adv. Mater.* **2003**, *15*, 1583–1594; c) J.-F. Gohy, *Adv. Polym. Sci.* **2005**, *190*, 65–136.

[2] a) Y. Mai, A. Eisenberg, *Chem. Soc. Rev.* **2012**, *41*, 5969–5985; b) L. Zhang, A. Eisenberg, *Science* **1995**, *268*, 1728–1731; c) P. A. Rupar, L. Chabanne, M. A. Winnik, I. Manners, *Science* **2012**, *337*, 559–562; d) J. Dua, R. K. O'Reilly, *Soft Matter* **2009**, *5*, 3544–3561; e) A. Blanazs, S. P. Armes, A. J. Ryan, *Macromol. Rapid Commun.* **2009**, *30*, 267–277; f) P. Tanner, P. Baumann, R. Enea, O. Onaca, C. Palivan, W. Meier, *Acc. Chem. Res.* **2011**, *44*, 1039–1049.

[3] R. Golan, L. I. Pietrasanta, W. Hasieh, H. G. Hansma, *Biochemistry* **1999**, *38*, 14069–14076.

[4] a) M. Allen, J. Lee, C. Lee, R. Balhorn, *Mol. Reprod. Dev.* **1996**, *45*, 87–92; b) M. Cerritelli, N. Cheng, A. Rosenberg, C. McPherson, F. Booy, A. Steven, *Cell* **1997**, *91*, 271–280; c) W. C. Earnshaw, J. King, S. C. Harrison, F. A. Eiserling, *Cell* **1978**, *14*, 559–568; d) N. V. Hud, M. J. Allen, K. H. Downing, J. Lee, R. Balhorn, *Biochem. Biophys. Res. Commun.* **1993**, *193*, 1347–1354; e) N. Hud, *Biophys. J.* **1995**, *69*, 1355–1362; f) S. Klimenko, T. Tikchonenko, V. Andreev, *J. Mol. Biol.* **1967**, *23*, 523–533; g) K. E. Richards, R. C. Williams, R. Calendar, *J. Mol. Biol.* **1973**, *78*, 255–259.

[5] a) E. Wagner, M. Cotten, R. Foisner, M. Birnstiel, *Proc. Natl. Acad. Sci. USA* **1991**, *88*, 4255–4259; b) A. Rolland, *Crit. Rev. Ther. Drug Carrier Syst.* **1998**, *15*, 143–198; c) C. Plank, M. X. Tang, A. R. Wolfe, F. C. Szoka, Jr., *Hum. Gene Ther.* **1999**, *10*, 319–332; d) R. Mahato, L. Smith, A. Rolland, *Adv. Genet.* **1999**, *41*, 95–155; e) D. Luo, W. Saltzman, *Nat. Biotechnol.* **2000**, *18*, 33–37; f) D. Kwoh, C. C. Coffin, C. P. Lollo, J. Jovenal, M. G. Banaszczyk, P. Mullen, A. Phillips, A. Amini, J. Fabrycki, R. Bartholomew, S. W. Brostoff, D. J. Carlo, *Biochim. Biophys. Acta Gene Struct. Expression* **1999**, *1444*, 171–190.

[6] a) K. Hales, Z. Chen, K. L. Wooley, D. J. Pochan, *Nano Lett.* **2008**, *8*, 2023–2026; b) H. Cui, Z. Chen, S. Zhong, K. L. Wooley, D. J. Pochan, *Science* **2007**, *317*, 647–650; c) Z. Li, E. Kesselman, Y. Talmon, M. A. Hillmyer, T. P. Lodge, *Science* **2004**, *306*, 98–101.

[7] D. J. Pochan, Z. Chen, H. Cui, K. Hales, K. Qi, K. L. Wooley, *Science* **2004**, *306*, 94–97.

[8] K. Yu, L. F. Zhang, A. Eisenberg, *Langmuir* **1996**, *12*, 5980–5984.

[9] a) J. Zhu, Y. Liao, W. Jiang, *Langmuir* **2004**, *20*, 3809–3812; b) S. Förster, N. Hermsdorf, W. Leube, H. Schnablegger, M. Regenbrecht, S. Akari, P. Lindner, C. Boettcher, *J. Phys. Chem. B* **1999**, *103*, 6657–6668; c) I. LaRue, M. Adam, M. Pitsikalis, N. Hadjichristidis, M. Rubinstein, S. S. Sheiko, *Macromolecules* **2006**, *39*, 309–314; d) I. C. Reynhout, J. J. L. M. Cornelissen, R. J. M. Nolte, *J. Am. Chem. Soc.* **2007**, *129*, 2327–2332; e) Y. L. Liu, Y. H. Chang, W. H. Chen, *Macromolecules* **2008**, *41*, 7857–7862; f) R. Hoogenboom, H. M. L. Thijs, D. Wouters, S. Hoeppener, U. S. Schubert, *Macromolecules* **2008**, *41*, 1581–1583; g) L. Liu, J. K. Kim, R. Gunawidjaja, V. V. Tsukruk, M. Lee, *Langmuir* **2008**, *24*, 12340–12346; h) C. Liu, G. Chen, H. Sun, J. Xu, Y. Feng, Z. Zhang, T. Wu, H. Chen, *Small* **2011**, *7*, 2721–2726; i) J. Fu, D. H. Kim, W. Knoll, *ChemPhysChem* **2009**, *10*, 1190–1194; j) X. Nie, J. Xu, J. Cui, B. Yang, W. Jiang, *RSC Adv.* **2013**, *3*, 24625–24633; k) Y. Zhang, X. Xiao, J.-J. Zhou, L. Wang, Z.-B. Li, L. Li, L.-Q. Shi, C.-M. Chan, *Polymer* **2009**, *50*, 6166–6171.

[10] a) B. E. M. Kenzie, S. J. Holder, N. A. J. M. Sommerdijk, *Curr. Opin. Colloid Interface Sci.* **2012**, *17*, 343–349; b) S. J. Holder, N. A. J. M. Sommerdijk, *Polym. Chem.* **2011**, *2*, 1018; c) A. G. Denkova, P. H. H. Bomans, M. O. Coppens, N. A. J. M. Sommerdijk, E. Mendes, *Soft Matter* **2011**, *7*, 6622–6628; d) U. Mansfeld, S. Hoeppener, K. Kempe, J.-M. Schumers, J.-F. Gohy, U. S. Schubert, *Soft Matter* **2013**, *9*, 5966–5974; e) B. E. McKenzie, F. Nudelman, P. H. H. Bomans, S. J. Holder, N. A. J. M. Sommerdijk, *J. Am. Chem. Soc.* **2010**, *132*, 10256–10259; f) A. L. Parry, P. H. H. Bomans, S. J. Holder, N. A. J. M. Sommerdijk, S. C. G. Biagini, *Angew. Chem. Int. Ed.* **2008**, *47*, 8859–8862; *Angew. Chem.* **2008**, *120*, 8991–8994; g) V. Percec, D. A. Wilson, P. Leowanawat, C. J. Wilson, A. D. Hughes, M. S. Kaucher, D. A. Hammer, D. H. Levine, A. J. Kim, F. S. Bates, K. P. Davis, T. P. Lodge, M. L. Klein, R. H. DeVane, E. Aqad, B. M. Rosen, A. O. Argintaru, M. J. Sienkowska, K. Rissanen, S. Nummelin, J. Ropponen, *Science* **2010**, *328*, 1009–1014; h) Z. Ju, J. He, *Chem. Commun.* **2014**, *50*, 8480–8483; i) Y. La, C. Park, T. J. Shin, S. H. Joo, S. Kang, K. T. Kim, *Nat. Chem.* **2014**, *6*, 534–541.

[11] a) B. E. McKenzie, J. F. de Visser, H. Friedrich, M. J. M. Wirix, P. H. H. Bomans, G. de With, S. J. Holder, N. A. J. M. Sommerdijk, *Macromolecules* **2013**, *46*, 9845–9848; b) H. Huang, B. Chung, J. Jung, H.-W. Park, T. Chang, *Angew. Chem. Int. Ed.* **2009**, *48*, 4594–4597; *Angew. Chem.* **2009**, *121*, 4664–4667.

[12] a) J. B. Gilroy, T. Gädt, G. R. Whittell, L. Chabanne, J. A. Mitchels, R. M. Richardson, M. A. Winnik, I. Manners, *Nat. Chem.* **2010**, *2*, 566–570; b) T. Gädt, N. S. Ieong, G. Cambridge, M. A. Winnik, I. Manners, *Nat. Mater.* **2009**, *8*, 144–150; c) J. A. Massey, K. Temple, L. Cao, Y. Rharbi, L. Raez, M. A. Winnik, I. Manners, *J. Am. Chem. Soc.* **2000**, *122*, 11577–11584; d) X. Wang, G. Guerin, H. Wang, Y. Wang, I. Manners, M. A. Winnik, *Science* **2007**, *317*, 644–647; e) A. Presa Soto, J. B. Gilroy, M. A. Winnik, I. Manners, *Angew. Chem. Int. Ed.* **2010**, *49*, 8220–8223; *Angew. Chem.* **2010**, *122*, 8396–8399.

[13] S. Suárez-Suárez, G. A. Carriedo, A. P. Soto, *Chem. Eur. J.* **2016**, *22*, 4483–4491.

[14] a) S. Wilfert, H. Henke, W. Schoefberger, O. Brüggemann, I. Teasdale, *Macromol. Rapid Commun.* **2014**, *35*, 1135–1141; b) A. P. Soto, I. Manners, *Macromolecules* **2009**, *42*, 40–42; c) S. Suárez-Suárez, D. Presa Soto, G. A. Carriedo, A. Presa Soto, A. Staubitz, *Organometallics* **2012**, *31*, 2571–2581; d) S. Suárez-Suárez, G. A. Carriedo, M. P. Tarazona, A. P. Soto, *Chem. Eur. J.* **2013**, *19*, 5644–5653; e) S. Suárez-Suárez, G. A. Carriedo, A. P. Soto, *Chem. Eur. J.* **2013**, *19*, 15933–15940; f) S. Suárez-Suárez, G. A. Carriedo, A. P. Soto, *Chem. Eur. J.* **2015**, *21*, 14129–14139.

[15] R. Prange, S. D. Reeves, H. R. Allcock, *Macromolecules* **2000**, *33*, 5763–5765.

[16] *Polymer Handbook*, *Vol. II* (Eds.: J. Brandrup, E. H. Immergut, E. A. Grulke), Wiley, New York, **1999**.

[17] Z. Yang, W. Zhang, J. Li, J. Chen, *Sep. Purif. Technol.* **2012**, *93*, 15–24.

[18] a) Z. Zhou, W. F. Edmons, M. A. Hillmyer, T. P. Lodge, *J. Am. Chem. Soc.* **2003**, *125*, 10182–10183; b) S. Zhu, W. F. Edmons, M. A. Hilmyer, T. P. Lodge, *J. Polym. Sci. Part B* **2005**, *43*, 3685–

3694; c) W. F. Edmonds, Z. Li, M. A. Hillmyer, T. P. Lodge, *Macromolecules* **2006**, *39*, 4526 – 4530.
[19] For selected examples of self-assembly studies with fluorine-containing blocks and the suggested formation of multicompartment micelles, see: a) K. Stähler, J. Selb, F. Candau, *Langmuir* **1999**, *15*, 7565 – 7576; b) R. Weberskirch, J. Preuschen, H. W. Spiess, O. Nuyken, *Macromol. Chem. Phys.* **2000**, *201*, 995 – 1007; c) P. Kujawa, C. C. E. Goh, D. Calvet, F. M. Winnik, *Macromolecules* **2001**, *34*, 6387 – 6395; d) A. Kotzev, A. Laschewsky, P. Adriaensens, J. Gelan, *Macromolecules* **2002**, *35*, 1091 – 1101.
[20] X. He, F. Schimid, *Phys. Rev. Lett.* **2008**, *100*, 137802.
[21] a) T. P. Russell, D. P. Anderson, R. S. Stein, C. R. Desper, J. J. Beres, N. S. Schneider, *Macromolecules* **1984**, *17*, 1795 – 1799; b) M. N. Alexander, C. R. Desper, P. L. Sagalyn, N. S. Schneider, *Macromolecules* **1977**, *10*, 721 – 723; c) M. Gleria, R. De Jaeger, *Phosphazenes: A Worldwide Insight*, Nova Science, New York, **2004**.

Received: May 31, 2016
Revised: June 20, 2016
Published online: July 26, 2016

